

Article

A Label-Free Fluorescent DNA Calculator Based on Gold Nanoparticles for Sensitive Detection of ATP

Jingjing Zhang, Shizhi Zhang, Chaoqun Niu, Chen Liu, Jie Du * and Yong Chen *

State Key Laboratory of Marine Resource Utilization in South China Sea, College of Information Science & Technology, College of Materials and Chemical Engineering, Institute of Tropical Agriculture and Forestry, Hainan University, Haikou 570228, China; zhangjingjingaoxue@163.com (J.Z.); 13698954926@163.com (S.Z.); chaoqunniu@163.com (C.N.); chen_liu@126.com (C.L.)

* Correspondence: dujie@hainu.edu.cn (J.D.); ychen2002@hainu.edu.cn (Y.C.)

Academic Editor: Marcel Hollenstein

Received: 6 September 2018; Accepted: 25 September 2018; Published: 29 September 2018



Abstract: Herein we described a deoxyribonucleic acid (DNA) calculator for sensitive detection of the determination of adenosine triphosphate (ATP) using gold nanoparticles (GNP) and PicoGreen fluorescence dye as signal transducer, and ATP and single-stranded DNA (DNA-M') as activators. The calculator-related performances including linearity, reaction time, logic gate, and selectivity were investigated, respectively. The results revealed that this oligonucleotide sensor was highly sensitive and selective. The detection range was 50–500 nmol/L ($R^2 = 0.99391$) and the detection limit was 46.5 nmol/L. The AND DNA calculator was successfully used for the ATP detection in human urine. Compared with other methods, this DNA calculator has the characteristics of being label-free, non-enzymic, simple, and highly sensitive.

Keywords: ATP detection; label-free fluorescence; enzyme-free; gold nanoparticles; DNA calculator

1. Introduction

Many diseases, such as Parkinson's disease, ischemia, hypoxia, hypoglycemia, and some malignant tumors, are closely related to the concentration of ATP [1–3]. Consequently, the detection of ATP is of substantial clinical importance. Methods based on fluorescent probes possess high sensitivity and selectivity as well as good compatibility with visible-light imaging of biological systems [4]. Accordingly, considerable efforts are being made to develop fluorescent sensors for the detection of ATP.

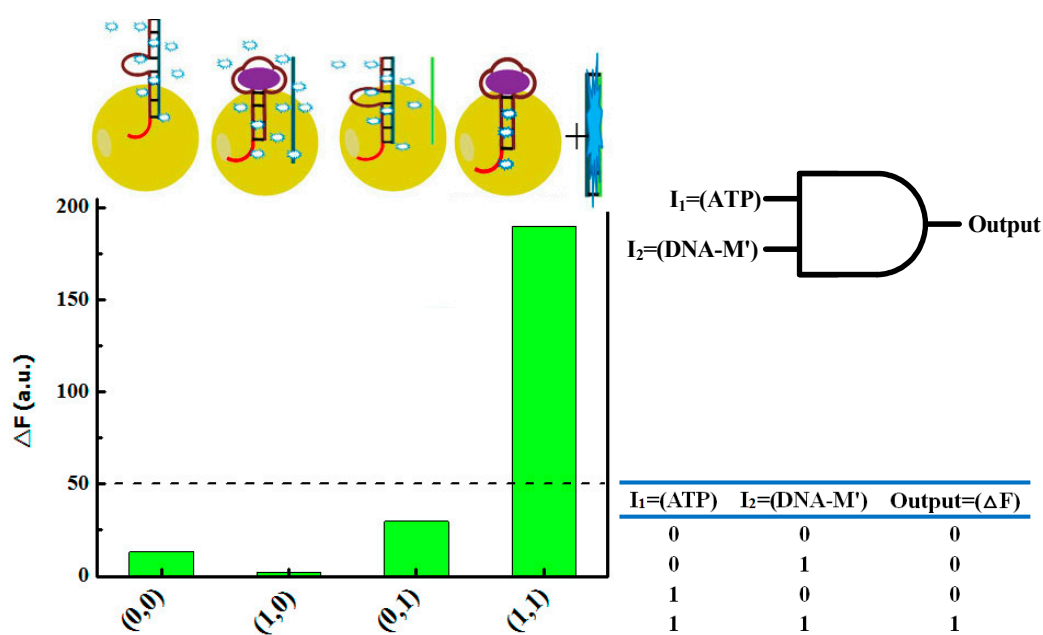
Signal amplification techniques, such as rolling circle replication [5] and strand displacement amplification [6–9], provide an effective strategy for improving the sensitivity of various biosensors. However, these methods usually suffer from a high background signal and often rely on the use of biological enzymes and fluorescent labels. Biological enzymes and fluorescent labels are typically expensive and sensitive to temperature and pH. Compared with signal amplification, the approach of background signal suppression is often simpler and requires a shorter reaction time [10,11]. Nanoparticles such as nanoceria [12] and gold nanoparticles (GNPs) [13,14] can be used as quenchers to suppress the background signal and enhance the sensor's sensitivity. However, most signal suppression approaches involve high cost due to fluorescence-labeled probe. To date, several label-free fluorescence methods, such as those based on the fluorescent dye probes thiazole orange [15], PicoGreen [16,17], and SYBR Green I [18], have been developed to detect ATP. However, neither signal amplification nor signal suppression was applied in most of these label-free fluorescence methods. In this study, we investigated the use of GNPs and the PicoGreen probe to construct a biosensor for ATP based on label-free fluorescence. The developed assay is simple, sensitive, and does not require enzymes and fluorescent label.

Molecular computers are very promising for applications in nanotechnology, medicine, and biotechnology. To date, certain math problems have been solved using DNA computers [19,20]. Molecular calculators can perform molecular Boolean operations. Although many molecular calculators, such as AND, INH + NINH, and INHIBIT [11,21,22], have been developed, there is still a need to construct DNA calculators that are more sensitive, simpler, and less expensive. The DNA calculator designed in this work has two different functions [23–30]. Firstly, this calculator is actually a kind of AND logic gate. Secondly, this DNA calculator can be used to sensitively determine and calculate ATP concentration based on the changes in fluorescence intensity. Hence, we constructed an AND DNA calculator based on label-free fluorescence using GNPs and PicoGreen, which is simple, enzyme-free, and highly sensitive. It is hoped that the general method developed in this work can be adopted for the detection of various different proteins and ions.

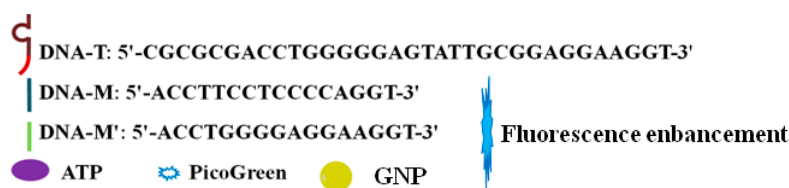
2. Results and Discussion

2.1. Establishment of AND DNA Calculator

Scheme 1 illustrates the operating principle of the GNP–PicoGreen-based AND DNA calculator for the detection of ATP. This assay exploits the properties of PicoGreen and GNPs. PicoGreen forms a highly luminescent complex upon binding dsDNA compared to binding ssDNA [16,17]. ssDNA and dsDNA (DNA-T + DNA-M) with a sticky end can adsorb onto the surfaces of GNPs at a particular ionic strength, enabling energy transfer to occur from the DNA to the GNPs and effectively quenching the fluorescence intensity [13]. However, the fully complementary dsDNA is released from the GNPs because it does not bind at the same ionic strength, and the PicoGreen fluorescence is observed. We used ssDNA (DNA-T) as an ATP-specific oligonucleotide and dsDNA (DNA-T + DNA-M) as the probe. The inputs are ATP and DNA-M' ssDNA, and the output is the fluorescence signal from PicoGreen. The presence of ATP and DNA-M' triggers the structural conversion of the probe from DNA-T + DNA-M dsDNA to DNA-M + DNA-M' dsDNA and induces a change in the PicoGreen fluorescence intensity. The presence of ATP or DNA-M' corresponds to input values of 1, whereas their absence corresponds to input values of 0. A high PicoGreen fluorescence intensity corresponds to an output value of 1, whereas a low fluorescence intensity corresponds to an output value of 0. As shown in Scheme 1, a strong output response occurs only when both ATP and DNA-M' are present (1,1), which is the Boolean calculation for an AND logic gate.



Scheme 1. Cont.



Scheme 1. Operating principle of the AND DNA calculator.

2.2. Assay Feasibility

Firstly, we used fluorescence spectroscopy to investigate the feasibility of the proposed assay. The differences between the peaks of the four curves and the peak of the a-curve in Figure 1 were used as the output signal, respectively. If the fluorescence intensity difference, ΔF , was greater than 50 a.u., the output signal was 1, otherwise it was 0. As shown in Figure 1, adsorption of the DNA-T + DNA-M dsDNA with sticky ends on the GNP surface (input 0,0) resulted in a strong quenching of the PicoGreen fluorescence owing to fluorescence resonance energy transfer (FRET) [13]. Upon the individual addition of ATP (1,0) or DNA-M' ssDNA (0,1), the fluorescence intensity barely changed because the dsDNA remained adsorbed on the GNP surface through the sticky end, resulting in FRET. However, the addition of both ATP and DNA-M' (1,1) resulted in the binding of ATP to DNA-T ssDNA and the release of DNA-M ssDNA, which subsequently bound to DNA-M' ssDNA to form DNA-M + DNA-M' dsDNA, causing an obvious increase in the fluorescence intensity due to binding of the PicoGreen to the DNA-M + DNA-M' dsDNA. This increase in the PicoGreen fluorescence intensity was induced only by the dual input of ATP and DNA-M', which conforms to the Boolean calculation of an AND logic gate as shown in Scheme 1.

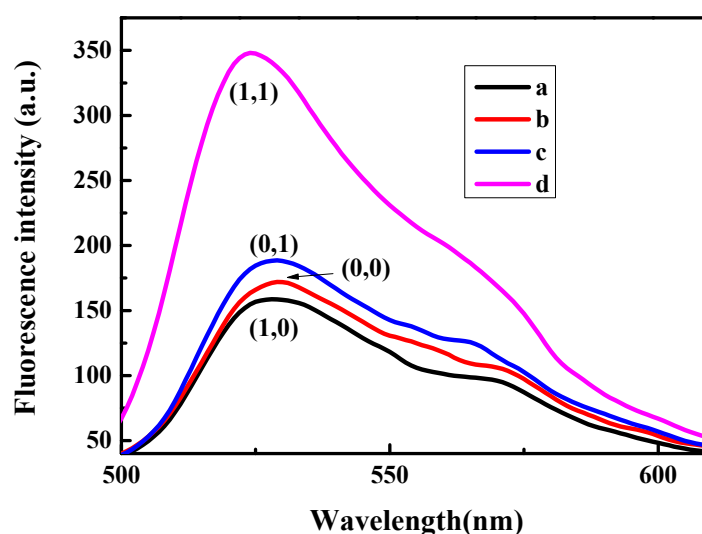


Figure 1. Fluorescence emission spectra: (a) DNA-T + DNA-M dsDNA, GNP and 200 μ L of 10 μ M ATP; (b) DNA-T + DNA-M dsDNA and GNP; (c) DNA-T + DNA-M dsDNA, GNP, and DNA-M'; (d) DNA-T + DNA-M dsDNA, GNP, DNA-M', and 200 μ L of 10 μ M ATP.

To further explore the feasibility of the assay principle, we monitored the reaction progress over time. Figure 2A shows that the fluorescence intensity decreased significantly when ATP was added to DNA-T + DNA-M dsDNA because the combination of ATP and DNA-T ssDNA led to the opening of the dsDNA complex [16]. Figure 2B demonstrates that the addition of GNP caused the fluorescence intensity to visibly decrease as a result of quenching [13,14]. The fluorescence intensity was weak upon the individual addition of ATP (1,0) or DNA-M' (0,1), as shown in Figures 2C and 2D, respectively. In contrast, the addition of both ATP and DNA-M' (1,1) resulted in a clear increase in the fluorescence

intensity. These results were consistent with those shown in Figure 1 and further demonstrate the feasibility of the proposed system.

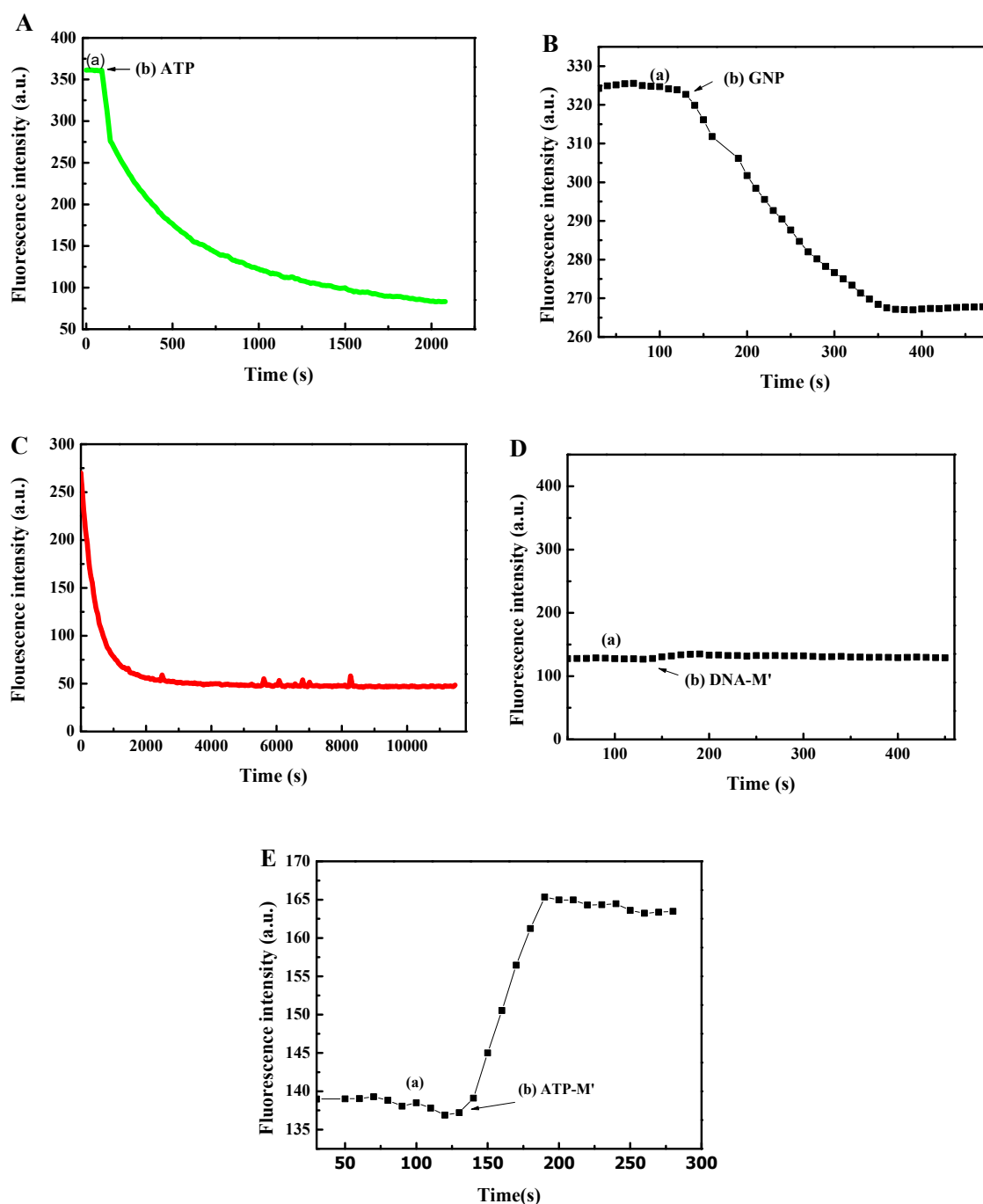


Figure 2. Monitoring of the reaction progress under various conditions: (A) (a) DNA-T + DNA-M dsDNA; (b) 200 μL of 10 μM ATP. (B) (a) DNA-T + DNA-M dsDNA; (b) GNP. (C) DNA-T + DNA-M dsDNA, GNP, and 200 μL of 10 μM ATP. (D) (a) DNA-T + DNA-M dsDNA and GNP; (b) DNA-M'. (E) (a) DNA-T + DNA-M dsDNA, GNP, and 200 μL of 10 μM ATP; (b) DNA-M'.

2.3. Assay Linearity and Sensitivity

The linearity and sensitivity were further examined by acquiring fluorescence spectra at various concentrations of ATP. Figure 3 shows that increasing the concentration of ATP from 50 to 500 nmol/L led to a linear increase in the relative change of fluorescence, demonstrating that the fluorescence

signal is strongly dependent on the ATP concentration. The linear regression equation was $y = 8.77379 \times 10^{-4}x - 0.01613$ (x and y refer to the ATP concentration and the relative change of fluorescence, respectively) with an R^2 value of 0.993, and the limit of detection (LOD) was 46.5 nmol/L ($3\sigma/\text{slope}$). Therefore, within this linear range, this equation can be used to quantitatively estimate the ATP concentration. Compared with most other methods (Table 1), the results clearly show that our method affords a lower detection limit and sufficient linearity and sensitivity for the detection of the target analyte ATP.

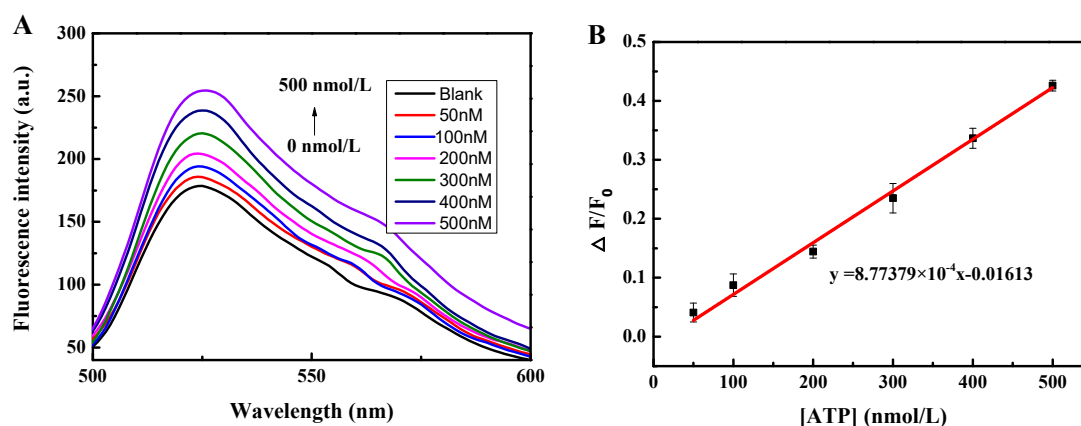


Figure 3. (A) Fluorescence emission spectra at various ATP concentrations. (B) Linearity for detection of ATP.

Table 1. Other methods for ATP detection.

Methods	LOD	Linear Range	Correlation Coefficient (R^2)	Reference
Graphene-Based Aptamer Logic Gates	2.07 $\mu\text{mol/L}$	5–50 $\mu\text{mol/L}$	0.997	23
Naphthalimide-rhodamine Compound (NR) probe	100 nmol/L	0.1–10 $\mu\text{mol/L}$	N/A	24
Oligonucleotide-templated Silver Nanoclusters	33 nmol/L	0.1–10 $\mu\text{mol/L}$	0.98	25
Core-Shell Ag@SiO ₂ Nanoflakes	8 $\mu\text{mol/L}$	0–0.5 mmol/L	N/A	26
DNA/Ag Nanoclusters	91.6 nmol/L	0.5–8.0 $\mu\text{mol/L}$	0.99	27
Gold Nanoclusters	43 $\mu\text{mol/L}$	50–100 $\mu\text{mol/L}$	0.9908	28
Carbon nanoparticles-Fe ³⁺	0.48 $\mu\text{mol/L}$	0.5–50 $\mu\text{mol/L}$	0.99733	29
ATP Displace Adsorbed DNA from Nanoceria	54 pmol/L	0.1 nmol/L–1.5 $\mu\text{mol/L}$	0.996	12
Magnetite Nanoparticle	30 nmol/L	100–1000 nmol/L	0.9950	30
GNP	46.5 nmol/L	50–500 nmol/L	0.99391	This work

2.4. Assay Selectivity

To assess the selectivity of the proposed sensing system, the responses of the assay to several similar control molecules (GTP, UTP, CTP, adenosine, ADP, and AMP) were evaluated under the same experimental conditions. Figure 4 shows that only negligible changes in fluorescence intensity occurred in the presence of these small molecules compared with a blank solution. However, the fluorescence intensity increased significantly in the presence of the target molecule ATP. Furthermore, the enhancement in fluorescence intensity caused by a mixture of these small molecules (ATP, GTP,

UTP, CTP, adenosine, ADP, and AMP) was similar to that caused by ATP alone. These results clearly demonstrate that the proposed assay has sufficient selectivity for the detection of ATP.

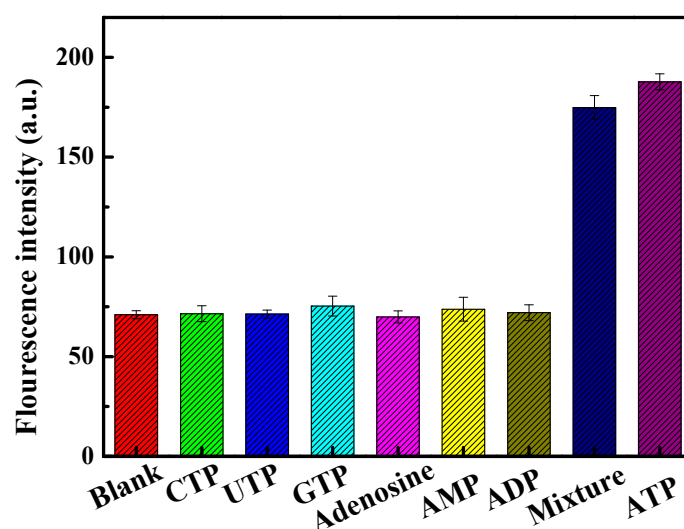


Figure 4. Selectivity of the assay for the detection of ATP. The mixture consists of ATP, CTP, UTP, GTP, adenosine, AMP, ADP, each in concentrations of 200 nmol/L.

2.5. Determination of ATP Concentration in Real Urine Samples

To validate the viability of the proposed assay, we conducted standard addition recovery tests by adding ATP to samples of human urine and serum. As shown in Table 2, the recovery rates of urine and serum samples were 98.4 to 101.4% and 101.2 to 103.6%, respectively. The experimental results were satisfactory, indicating that the proposed method is reliable and has immense potential for determining the ATP concentration not only in real urine but also in serum samples, which endow this proposed system more significant for the practical application.

Table 2. Detection of ATP concentration in the real samples of urine and serum.

Samples	ATP		Proposed Recovery (%)	Method	
	Added	Found		SD ($n = 3$)	RSD ($n = 3$)
	(nmol/L)	(nmol/L)		(nmol/L)	(%)
Urine-1	100.00	99.9749	98.4	1.2	1.2
		97.0575			
		98.1570			
Urine-2	300.00	295.1230	101.4	6.65	2.7
		305.9749			
		311.0817			
Urine-3	500.00	513.4384	99.2	13.2	2.6
		492.3729			
		481.5200			
Serum-1	100.00	110.8895	103.6	5.3	5.2
		98.1786			
		101.8063			
Serum-2	300.00	299.0586	101.3	4.1	1.3
		301.0191			
		303.8109			
Serum-3	500.00	506.5864	101.2	5.6	1.1
		498.6701			
		502.3293			

3. Materials and Methods

3.1. Materials and Reagents

Adenosine, adenosine diphosphate (ADP), adenosine monophosphate (AMP), Cytidine triphosphate (CTP), ATP, guanosine triphosphate (GTP), uridine triphosphate (UTP), and PicoGreen dye were supplied by Shanghai Yi Sheng Technology Co., Ltd. (Shanghai, China). All oligonucleotides were purchased from Beijing Genomics Institute (Beijing, China). The DNA sequences are listed in Table 3. PicoGreen dsDNA quantitation reagent was purchased from Shanghai Yi Sheng Biotechnology Co., Ltd. (Shanghai, China). GNP was purchased from the Lianshi Mall (Beijing, China).

All reagents were diluted in buffer solution (10 mmol/L Tris, 10 mmol/L MgCl₂, 50 mmol/L NaCl, pH 7.5). The volumes of buffer solution, PicoGreen (200-fold dilution), double-stranded DNA (dsDNA), single-stranded DNA (ssDNA), and GNPs (10-fold dilution) were 1800 µL, 30 µL, 90 µL, 100 µL, and 10 µL, respectively, in all experiments. Components in each experiments illustrated in Figures 1 and 2 are listed in Tables 4 and 5, respectively.

Table 3. DNA sequences.

Oligonucleotide	Sequence
DNA-T	5'-CGC GCG ACC TGG GGG AGT ATT GCG GAG GAA GGT-3'
DNA-M	5'-ACC TTC CTC CCC AGG T-3'
DNA-M'	5'-ACC TGG GGA GGA AGG T-3'

Table 4. Components in the experiment of Figure 1.

Name	Components
a-curve	1800 µL buffer, 30 µL PicoGreen, 90 µL DNA-T + DNA-M dsDNA, 10 µL GNP, 200 µL of 10 µM ATP
b-curve	1800 µL buffer, 30 µL PicoGreen, 90 µL DNA-T + DNA-M dsDNA and 10 µL GNP
c-curve	1800 µL buffer, 30 µL PicoGreen, 90 µL DNA-T + DNA-M dsDNA and 10 µL GNP, 100 µL DNA-M'
d-curve	1800 µL buffer, 30 µL PicoGreen, 90 µL DNA-T + DNA-M dsDNA and 10 µL GNP, 100 µL DNA-M', 200 µL of 10 µM ATP

Table 5. Components in the experiment of Figure 2.

Name	Components
Figure 2A	(a) 1800 µL buffer, 30 µL PicoGreen, 90 µL DNA-T + DNA-M dsDNA
	(b) 200 µL of 10 µM ATP
Figure 2B	(a) 1800 µL buffer, 30 µL PicoGreen, 90 µL DNA-T + DNA-M dsDNA
	(b) 10 µL GNP
Figure 2C	1800 µL buffer, 30 µL PicoGreen, 90 µL DNA-T + DNA-M dsDNA, 10 µL GNP, 200 µL of 10 µM ATP
Figure 2D	(a) 1800 µL buffer, 30 µL PicoGreen, 90 µL DNA-T + DNA-M dsDNA, 10 µL GNP
	(b) 100 µL DNA-M'
Figure 2E	(a) 1800 µL buffer, 30 µL PicoGreen, 90 µL DNA-T + DNA-M dsDNA, 10 µL GNP, 200 µL of 10 µM ATP
	(b) 100 µL DNA-M'

3.2. Apparatus

The fluorescence spectra and reaction progress were measured using a fluorescence spectrometer (RF-6000, Shimadzu, Tokyo, Japan). The fluorescence spectra were acquired with an excitation wavelength of 480 nm and a detection range from 495 to 700 nm. The reaction progress was monitored using an excitation wavelength of 480 nm and an emission wavelength of 520 nm.

3.3. ATP Detection in Real Samples

Fresh human serum samples were supplied by Nanjing China Senbeijia Biological Technology Co., Ltd., which did not do any other pretreatment. We obtained urine from a healthy adult and did not add any detergent. The urine sample was centrifuged at 12,000 rpm for 2 min and the supernatant was diluted tenfold with buffer solution. ATP was then added to the diluted urine and fresh human serum samples at concentrations of 100, 300, and 500 nmol/L, and each measurement was performed in triplicate. Finally, the ATP recovery was calculated.

4. Conclusions

We developed a label-free-fluorescence-based and enzyme-free AND DNA calculator for the sensitive and convenient determination of ATP concentration. This AND DNA calculator has many important features. First, the GNP-based DNA calculator partially eliminates the background signal and improves the sensitivity of the sensor. Second, this DNA calculator does not require fluorescent labeling or enzymes, leading to a lower assay cost. Third, this DNA calculator is highly selective for ATP in the presence of similar small molecules (GTP, UTP, and CTP) and affords a lower detection limit compared with most of the previously reported methods. Most importantly, this DNA calculator can be successfully applied to the detection of ATP in urine samples, demonstrating its immense potential for practical clinical diagnosis. Owing to these advantages, the proposed method could also be extended to facilitate the detection of other small molecules and proteins in a label-free and enzyme-free manner.

Author Contributions: J.Z. and S.Z. performed the experiments and wrote the paper; C.N. and C.L. analyzed the data; J.D. and Y.C. conceived and designed the experiments.

Funding: This research was funded by the Hainan Provincial Natural Science Foundation of China (Grant No. 518QN215, 2018CXTD332), the National Nature Science Foundation of China (Grant No. 21763009), and Hainan Province graduate student innovative research projects (Grant No. Hys2018-59, Hys2018-60).

Conflicts of Interest: The authors declare no conflict of interest.

References

1. Aw, T.Y.; Jones, D.P. Atp concentration gradients in cytosol of liver cells during hypoxia. *Am. J. Physiol.* **1985**, *249*, C385–C392. [[CrossRef](#)] [[PubMed](#)]
2. Agardh, C.D.; Folbergrova, J.; Siesjo, B.K. Cerebral metabolic changes in profound, insulin-induced hypoglycemia, and in the recovery period following glucose administration. *J. Neurochem.* **1978**, *31*, 1135–1142. [[CrossRef](#)] [[PubMed](#)]
3. Katsura, K.; Folbergrova, J.; Bengtsson, F.; Kristian, T.; Gido, G.; Siesjo, B.K. Recovery of mitochondrial and plasma membrane function following hypoglycemic coma: Coupling of ATP synthesis, K⁺ transport, and changes in extra- and intracellular pH. *J. Cereb. Blood Flow Metab.* **1993**, *13*, 820–826. [[CrossRef](#)] [[PubMed](#)]
4. Xiao, L.; Sun, S.; Pei, Z.; Pei, Y.; Pang, Y.; Xu, Y. A Ga³⁺ self-assembled fluorescent probe for ATP imaging in vivo. *Biosens. Bioelectron.* **2015**, *65*, 166–170. [[CrossRef](#)] [[PubMed](#)]
5. Zhou, F.; Li, B.; Ma, J. A linear DNA probe as an alternative to a molecular beacon for improving the sensitivity of a homogenous fluorescence biosensing platform for DNA detection using target-primed rolling circle amplification. *RSC Adv.* **2015**, *5*, 4019–4025. [[CrossRef](#)]
6. Chen, H.G.; Ren, W.; Jia, J.; Feng, J.; Gao, Z.F.; Li, N.B.; Luo, H.Q. Fluorometric detection of mutant DNA oligonucleotide based on toehold strand displacement-driving target recycling strategy and exonuclease III-assisted suppression. *Biosens. Bioelectron.* **2016**, *77*, 40–45. [[CrossRef](#)] [[PubMed](#)]

7. Wang, X.P.; Yin, B.C.; Wang, P.; Ye, B.C. Highly sensitive detection of micrnas based on isothermal exponential amplification-assisted generation of catalytic g-quadruplex dnzyme. *Biosens. Bioelectron.* **2013**, *42*, 131–135. [[CrossRef](#)] [[PubMed](#)]
8. Huang, J.; Su, X.; Li, Z. Enzyme-free and amplified fluorescence DNA detection using bimolecular beacons. *Anal. Chem.* **2012**, *84*, 5939–5943. [[CrossRef](#)] [[PubMed](#)]
9. Zhang, D.Y.; Winfree, E. Control of DNA strand displacement kinetics using toehold exchange. *J. Am. Chem. Soc.* **2009**, *131*, 17303–17314. [[CrossRef](#)] [[PubMed](#)]
10. Liu, X.; Yang, Y.; Hua, X.; Feng, X.; Su, S.; Huang, Y.; Fan, Q.; Wang, L.; Huang, W. An improved turn-on aptasensor for thrombin detection using split aptamer fragments and graphene oxide. *Chin. J. Chem.* **2015**, *33*, 981–986. [[CrossRef](#)]
11. Lv, H.; Li, S.; Liu, Y.; Wang, G.; Li, X.; Lu, Y.; Wang, J. A reversible fluorescent inhibit logic gate for determination of silver and iodide based on the use of graphene oxide and a silver-selective probe DNA. *Microchim. Acta* **2015**, *182*, 2513–2520. [[CrossRef](#)]
12. Li, F.; Hu, X.; Wang, F.; Zheng, B.; Du, J.; Xiao, D. A fluorescent “on-off-on” probe for sensitive detection of ATP based on ATP displacing DNA from nanoceria. *Talanta* **2018**, *179*, 285–291. [[CrossRef](#)] [[PubMed](#)]
13. Jin, Y.; Li, H.; Bai, J. Homogeneous selecting of a quadruplex-binding ligand-based gold nanoparticle fluorescence resonance energy transfer assay. *Anal. Chem.* **2009**, *81*, 5709–5715. [[CrossRef](#)] [[PubMed](#)]
14. Yin, B.C.; Zuo, P.; Huo, H.; Zhong, X.; Ye, B.C. Dnzyme self-assembled gold nanoparticles for determination of metal ions using fluorescence anisotropy assay. *Anal. Biochem.* **2010**, *401*, 47–52. [[CrossRef](#)] [[PubMed](#)]
15. Kang, B.H.; Gao, Z.F.; Li, N.; Shi, Y.; Li, N.B.; Luo, H.Q. Thiazole orange as a fluorescent probe: Label-free and selective detection of silver ions based on the structural change of i-motif DNA at neutral ph. *Talanta* **2016**, *156–157*, 141–146. [[CrossRef](#)] [[PubMed](#)]
16. Lv, Z.; Liu, J.; Zhou, Y.; Guan, Z.; Yang, S.; Li, C.; Chen, A. Highly sensitive fluorescent detection of small molecules, ions, and proteins using a universal label-free aptasensor. *Chem. Commun.* **2013**, *49*, 5465–5467. [[CrossRef](#)] [[PubMed](#)]
17. Dragan, A.I.; Casas-Finet, J.R.; Bishop, E.S.; Strouse, R.J.; Schenerman, M.A.; Geddes, C.D. Characterization of picogreen interaction with dsdna and the origin of its fluorescence enhancement upon binding. *Biophys. J.* **2010**, *99*, 3010–3019. [[CrossRef](#)] [[PubMed](#)]
18. Pu, W.; Zhao, H.; Huang, C.; Wu, L.; Xua, D. Fluorescent detection of silver(i) and cysteine using sybr green i and a silver(i)-specific oligonucleotide. *Microchim. Acta* **2012**, *177*, 137–144. [[CrossRef](#)]
19. Braich, R.S.; Chelyapov, N.; Johnson, C.; Rothmund, P.W.K.; Adleman, L. Solution of a 20-variable 3-sat problem on a DNA computer. *Science* **2002**, *296*, 499–502. [[CrossRef](#)] [[PubMed](#)]
20. Benenson, Y.; Paz-Elizur, T.; Adar, R.; Keinan, E.; Livneh, Z.; Shapiro, E. Programmable and autonomous computing machine made of biomolecules. *Nature* **2001**, *414*, 430–434. [[CrossRef](#)] [[PubMed](#)]
21. Li, J.; Huang, Y.Q.; Qin, W.S.; Liu, X.F.; Huang, W. An optical-logic system based on cationic conjugated polymer/DNA/intercalating dyes assembly for label-free detection of conformational conversion of DNA i-motif structure. *Polym. Chem.* **2011**, *2*, 1341. [[CrossRef](#)]
22. Zhao, Y.; Zhang, Q.; Wang, W.; Jin, Y. Input-dependent induction of g-quadruplex formation for detection of lead (ii) by fluorescent ion logic gate. *Biosens. Bioelectron.* **2013**, *43*, 231–236. [[CrossRef](#)] [[PubMed](#)]
23. Shi, F.; Li, Y.; Lin, Z.; Ma, D.; Su, X. A novel fluorescent probe for adenosine 5'-triphosphate detection based on Zn²⁺-modulated l-cysteine capped cdte quantum dots. *Sens. Actuators B Chem.* **2015**, *220*, 433–440. [[CrossRef](#)]
24. Tang, J.L.; Li, C.Y.; Li, Y.F.; Zou, C.X. A ratiometric fluorescent probe with unexpected high selectivity for ATP and its application in cell imaging. *Chem. Commun.* **2014**, *50*, 15411–15414. [[CrossRef](#)] [[PubMed](#)]
25. Lee, J.D.; Cang, J.; Chen, Y.C.; Chen, W.Y.; Ou, C.M.; Chang, H.T. Detection of adenosine 5'-triphosphate by fluorescence variation of oligonucleotide-templated silver nanoclusters. *Biosens. Bioelectron.* **2014**, *58*, 266–271. [[CrossRef](#)] [[PubMed](#)]
26. Lu, L.; Qian, Y.; Wang, L.; Ma, K.; Zhang, Y. Metal-enhanced fluorescence-based core-shell Ag@SiO₂ nanoflares for affinity biosensing via target-induced structure switching of aptamer. *ACS Appl. Mater. Interfaces* **2014**, *6*, 1944–1950. [[CrossRef](#)] [[PubMed](#)]
27. Zhu, Y.; Hu, X.C.; Shi, S.; Gao, R.R.; Huang, H.L.; Zhu, Y.Y.; Lv, X.Y.; Yao, T.M. Ultrasensitive and universal fluorescent aptasensor for the detection of biomolecules (ATP, adenosine and thrombin) based on DNA/Ag nanoclusters fluorescence light-up system. *Biosens. Bioelectron.* **2016**, *79*, 205–212. [[CrossRef](#)] [[PubMed](#)]

28. Li, P.H.; Lin, J.Y.; Chen, C.T.; Ciou, W.R.; Chan, P.H.; Luo, L.; Hsu, H.Y.; Diao, E.W.; Chen, Y.C. Using gold nanoclusters as selective luminescent probes for phosphate-containing metabolites. *Anal. Chem.* **2012**, *84*, 5484–5488. [[CrossRef](#)] [[PubMed](#)]
29. Zhan, Z.; Cai, J.; Wang, Q.; Su, Y.; Zhang, L.; Lv, Y. Green synthesis of fluorescence carbon nanoparticles from yam and application in sensitive and selective detection of ATP. *Luminescence* **2016**, *31*, 626–632. [[CrossRef](#)] [[PubMed](#)]
30. Yu, C.J.; Wu, S.M.; Tseng, W.L. Magnetite nanoparticle-induced fluorescence quenching of adenosine triphosphate-bodipy conjugates: Application to adenosine triphosphate and pyrophosphate sensing. *Anal. Chem.* **2013**, *85*, 8559–8565. [[CrossRef](#)] [[PubMed](#)]

Sample Availability: Samples of the compounds ATP, GNP, and PicoGreen fluorescence dye are available from the authors.



© 2018 by the authors. Licensee MDPI, Basel, Switzerland. This article is an open access article distributed under the terms and conditions of the Creative Commons Attribution (CC BY) license (<http://creativecommons.org/licenses/by/4.0/>).